

# Hybrid Force/Position Control of a Very Flexible Parallel Robot Manipulator in Contact with an Environment

Fatemeh Ansarieshlaghi<sup>a</sup> and Peter Eberhard<sup>b</sup>

*Institute of Engineering and Computational Mechanics, University of Stuttgart,  
Pfaffenwaldring 9, 70569 Stuttgart, Germany*

**Keywords:** Flexible Parallel Robot, Position Control, Force Control, Impedance Control.

**Abstract:** There are many applications for robot manipulators and these tasks are complicated when they have interaction with environments and humans. This paper investigates a novel strategy to control a very flexible parallel manipulator interacting with an environment. The controller is complicated when the used robot manipulator is a flexible multibody dynamics system and the flexibility shall be taken into account in the modeling and controlling process. Also, interaction with an unknown environment is another challenge of our research. Hence, a sophisticated controller is designed to overcome the respective challenges. To this end, a hybrid force/position control strategy is utilized. Therefore, two controllers based on the rigid and flexible models of the robot are designed and implemented to interact with a surface. The simulation results show that the controllers based on the flexible model have a better performance than those based on the rigid model and successfully track a trajectory and interact with an environment.


## 1 INTRODUCTION


Light-weight manipulators attract a lot of research interest because of their complementing advantages. The advantages of light-weight robots include low energy usage, less mass, and often high working speeds. However, due to the light-weight design, the bodies have a significant flexibility which yields undesired deformations and vibrations. These manipulators can be modeled as flexible multibody systems and their flexibility must be taken into account in the controller design. The flexible multibody system with significant deformations complicates the control design because there are more generalized coordinates than control inputs. This complicated controller has a more complex design when the robot interacts with an environment. The controller shall be able to regulate the interaction force and move along the surface at the same time. In order to obtain a high performance in the end-effector's contact part, an accurate and efficient model as well as a nonlinear controller is necessary.

In this research, to investigate the controller a flexible robot available in hardware in our laboratory is

used. This robot has a  $\lambda$ -shape and its links are very flexible. In previous researches on this robot, only its modeling and position control were investigated. The modeling is described in (Burkhardt et al., 2013a). Also, an experimental study on the modeling and the modeling improvement were done in (Burkhardt et al., 2014) and (Ansarieshlaghi and Eberhard, 2017). The position control of this system can be done by a model-based or non-model-based feedback controller. Non-model-based feedback controllers in joint space were investigated in (Burkhardt et al., 2014) and (Morlock et al., 2016) and the flexible model based nonlinear feedback controller in joint space was investigated in (Ansarieshlaghi and Eberhard, 2018b). An experimental study of the rigid model-based controller on the lambda robot in the workspace was also done in (Morlock et al., 2017).

In contrast, in the previous works, here, a feedback controller of the lambda robot in work space is desired. Also, a part as a contact force regulator is added to the position controller in order to control the interaction with an environment. For interacting with an environment, control of the contact force in the interactive part is required. There are two methods to control this force, i.e., direct and indirect contact force control methods. In the direct approach, the controller regulates the force with a control loop and

<sup>a</sup>  <https://orcid.org/0000-0003-2693-0882>

<sup>b</sup>  <https://orcid.org/0000-0003-1809-4407>

using feedback of the force measurement and desired value of the force. For this method, an explicit model of the interaction environment is required, see (Luh et al., 1983). In the indirect force control methods, the force is controlled via position controller as an impedance (Hogan, 1985).

The contact force control of the light weight robots is very important task and there are many applications on this topic, e.g., industrial (Schindlbeck and Haddadin, 2015; Suarez et al., 2018), surgical (Li et al., 2018; Sandoval et al., 2018; Kamikawa et al., 2018), or soft robotic application (Vogel et al., 2015). Also, the contact force control of a flexible robot is investigated with one flexible link in (Endo et al., 2017; Feliu-Talegon et al., 2019) and for multi flexible links in (Suarez et al., 2018).

In our research, a hybrid force/position control is designed using the impedance controller approach (Siciliano and Khatib, 2016; Jung et al., 2004) for a very flexible robot manipulator.

The novelty of this work is that a nonlinear flexible model based position controller of the lambda robot in workspace is designed. Then, this position controller is combined with an impedance part in order to have a controller architecture that can be used for controlling the position and acting force of the end-effector's contact part during its interaction with an environment. The impedance part computes a new end-effector position based on the measured or estimated force and the position of the end-effector. Therefore, the impedance part generates a new end-effector position for tracking by the position controller part.

The nonlinear flexible model based controller in Cartesian space is simulated and compared with the rigid model based one. To test the designed pure position controller, the end-effector tracks a trajectory with low and high speed. Comparison results show that the flexible model based controller can track a trajectory with much higher accuracy than the rigid based and it shows very high tracking performance. To investigate the hybrid force/position controller, the end-effector's contact part interacts with a flat surface in two scenarios, interaction with a known and an unknown environment. Simulation results on the lambda robot show that the flexible based controller has better performance than the rigid based for both scenarios and the robot using this flexible based impedance controller can apply the desired force during moving along the surface with high accuracy.

The paper is organized as follows: Section 2 describes the robot, i.e., its mechanical and electrical parts. Section 3 includes the modeling of the flexible parallel lambda robot. Section 4 explains the ar-

chitecture of the nonlinear controller, i.e., the position controller and impedance controller. In Section 5, the proposed nonlinear controller is simulated and the results are discussed.

## 2 FLEXIBLE LAMBDA ROBOT

The used lambda robot is a simple parallel robot manipulator. This robot has highly flexible links. The end of the short link is connected in the middle of the long link using rigid bodies. This connection creates a closed loop kinematics constraint that causes the parallel configuration of the robot. This robot has two prismatic actuators connecting the links to the ground. The links are connected using passive revolute joints to the linear actuators. Another revolute joint is used to connect the short link and the middle of the long link. An additional rigid body is attached to the free end of the long link as an end-effector. The drive positions and velocities are measured with two optical encoders. Three full Wheatstone bridge strain gauge sets are attached on the long flexible link to measure its deformation. The lambda robot configuration shown in Figure 1 has been built in hardware, see (Burkhardt et al., 2014) at the Institute of Engineering and Computational Mechanics of the University of Stuttgart.

The electrical part of the hardware includes some power supplies for motors, strain gauge's amplifiers, digital/analog input-outputs boards, one *Speedgoat* target, a host computer, etc. For controlling the robot, the online control is done with a *Speedgoat* performance real-time target machine running a *Mathworks xPCtarget* kernel, which is called *Simulink Real-Time* since *Matlab R2014a*. Also, to observe the controller progress a graphical user interface is available for the input, output, safety logic of the lambda robot and their communication.

## 3 MODELING OF THE FLEXIBLE LAMBDA ROBOT

The modeling process of the flexible manipulator with  $\lambda$  configuration can be separated into three major steps. First, the flexible components of the system are modeled with the linear finite element method in the commercial finite element code *ANSYS*. Next, in order to control the  $\lambda$  robot, the degrees of freedom of the flexible bodies are reduced. Therefore, model order reduction is utilized. Then, all the rigid and flexible parts are modeled as a flexible multibody system

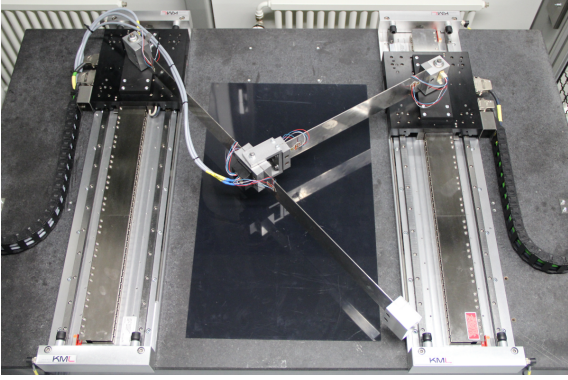


Figure 1: Mechanical setup of the flexible parallel lambda robot.

with a kinematic loop using the generalized coordinates  $\mathbf{q} \in \mathbb{R}^5$  as

$$\mathbf{M}(\mathbf{q})\ddot{\mathbf{q}} = \mathbf{f}(\mathbf{q}, \dot{\mathbf{q}}) + \mathbf{B}(\mathbf{q})\mathbf{u} + \mathbf{C}^T(\mathbf{q})\boldsymbol{\lambda}, \quad (1a)$$

$$\mathbf{c}(\mathbf{q}) = \mathbf{0}. \quad (1b)$$

The symmetric, positive definite mass matrix  $\mathbf{M} \in \mathbb{R}^{5 \times 5}$  depends on the joint angles and the elastic coordinates. The vector  $\mathbf{f} \in \mathbb{R}^5$  contains the generalized centrifugal, Coriolis and Euler forces, and the vector of applied forces and inner forces due to the body elasticity. The input matrix  $\mathbf{B} \in \mathbb{R}^{5 \times 2}$  maps the input vector  $\mathbf{u} \in \mathbb{R}^2$  to the system. The constraint equations are defined by  $\mathbf{c} \in \mathbb{R}^2$ . The Jacobian matrix of the constraint  $\mathbf{C} = \partial \mathbf{c}(\mathbf{q}) / \partial \mathbf{q} \in \mathbb{R}^{2 \times 5}$  maps the reaction force  $\boldsymbol{\lambda} \in \mathbb{R}^2$  due to the kinematic loop.

The flexible lambda robot is modeled as a flexible multibody system in *Neweul-M<sup>2</sup>* (Burkhardt et al., 2013b). The simulated model of the lambda robot is shown in Figure 2, see also (Burkhardt et al., 2013a; Ansarieshlaghi and Eberhard, 2018a).

While the system has a kinematics loop as a constraint in Equation (1b), the system accelerations  $\ddot{\mathbf{q}}$  can be divided into dependent  $\ddot{\mathbf{q}}_d \in \mathbb{R}^2$  and independent  $\ddot{\mathbf{q}}_i \in \mathbb{R}^3$  coordinates and the system constraints can be written as

$$\ddot{\mathbf{c}} = \mathbf{C}\ddot{\mathbf{q}} + \mathbf{c}'' = \mathbf{C}_i\ddot{\mathbf{q}}_i + \mathbf{C}_d\ddot{\mathbf{q}}_d + \mathbf{c}'' \quad (2)$$

where  $\mathbf{q}_d = [\alpha_1, \alpha_2]^T$ ,  $\mathbf{q}_i = [s_1, s_2, q_e]^T$ ,  $\mathbf{C}_d$  and  $\mathbf{C}_i$  are dependent and independent parts of the Jacobian matrix of the constraint and  $\mathbf{c}''$  presents local accelerations due to the constraints. The parameter  $q_e$  describes elastic coordinates of the flexible long link. Based on Equation (2), the system's generalized acceleration can be formulated as

$$\ddot{\mathbf{q}} = \begin{bmatrix} \ddot{\mathbf{q}}_i \\ \ddot{\mathbf{q}}_d \end{bmatrix} = \begin{bmatrix} \mathbf{I}_{3 \times 3} \\ -\mathbf{C}_d^{-1}\mathbf{C}_i \end{bmatrix} \ddot{\mathbf{q}}_i + \begin{bmatrix} \mathbf{0}_3 \\ -\mathbf{C}_d^{-1}\mathbf{c}'' \end{bmatrix} = \mathbf{J}_c\ddot{\mathbf{q}}_i + \mathbf{b}'' \quad (3)$$

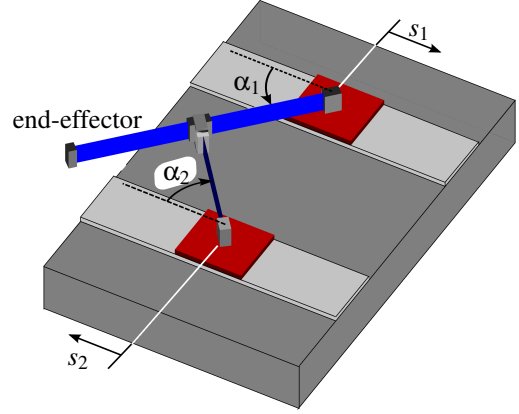


Figure 2: Mechanical model of flexible parallel robot.

Here,  $\mathbf{J}_c$  and  $\mathbf{b}''$  are Jacobian matrix and local accelerations due to rewriting the generalized acceleration based on the system constraints. Finally, by left-side multiplication with the transposed of the Jacobian matrix  $\mathbf{J}_c$  and replacing  $\ddot{\mathbf{q}}$  by Equation (3), Equation (1a) can be written as

$$\mathbf{J}_c^T \mathbf{M}(\mathbf{J}_c\ddot{\mathbf{q}}_i + \mathbf{b}'') = \mathbf{J}_c^T (\mathbf{f} + \mathbf{B}\mathbf{u} + \mathbf{C}^T(\mathbf{q})\boldsymbol{\lambda}) \quad (4)$$

while the multiplication matrix of the rewritten Jacobian matrix and the Jacobian matrix of the constraint is  $\mathbf{J}_c^T \mathbf{C}^T = \mathbf{0}$ , the equation of motion (1a) can be determined, see (Burkhardt et al., 2013a), by

$$\bar{\mathbf{M}}\ddot{\mathbf{q}}_i = \bar{\mathbf{f}} + \bar{\mathbf{B}}\mathbf{u}. \quad (5)$$

In Equation (5), the inertia matrix  $\bar{\mathbf{M}} \in \mathbb{R}^{3 \times 3}$  is  $\mathbf{J}_c^T \mathbf{M} \mathbf{J}_c$ , the input matrix  $\bar{\mathbf{B}} \in \mathbb{R}^{3 \times 2}$  is  $\mathbf{J}_c^T \mathbf{B}$ , and the vector  $\bar{\mathbf{f}} \in \mathbb{R}^3$  is  $\mathbf{J}_c^T (\mathbf{M}\mathbf{b}'' + \mathbf{f})$  from Equation (4). The independent generalized acceleration can be obtained by

$$\ddot{\mathbf{q}}_i = \bar{\mathbf{M}}^{-1}(\bar{\mathbf{f}} + \bar{\mathbf{B}}\mathbf{u}). \quad (6)$$

Equation (6) will be used for the workspace description of the system dynamics and designing the nonlinear feedback controller.

## Joint Space to Work Space Transformation

The system kinematics is formulated as

$$\mathbf{x} = \mathbf{s}(\mathbf{q}_i), \quad (7)$$

where  $\mathbf{x} \in \mathbb{R}^2$  is the end-effector position and  $\mathbf{s} \in \mathbb{R}^2$  is a nonlinear function of the independent system coordinates  $\mathbf{q}_i$ . The velocity and acceleration of the end-effector in the Cartesian space are calculated by the time derivative of the end-effector position function in Equation (7) by

$$\dot{\mathbf{x}} = \mathbf{J}\dot{\mathbf{q}}_i, \quad (8a)$$

$$\ddot{\mathbf{x}} = \mathbf{J}\ddot{\mathbf{q}}_i + \dot{\mathbf{J}}\dot{\mathbf{q}}_i, \quad (8b)$$

In Equation (8b),  $\mathbf{J}$  and  $\dot{\mathbf{J}}$  are the Jacobian matrix of the robot kinematics and its derivative. Finally, by replacing  $\dot{\mathbf{q}}_i$  from Equation (6) to Equation (8b), the dynamics description can be found in workspace coordinates with

$$\ddot{\mathbf{x}} = \mathbf{J}(\bar{\mathbf{M}}^{-1}(\bar{\mathbf{f}} + \bar{\mathbf{B}}\mathbf{u})) + \dot{\mathbf{J}}\dot{\mathbf{q}}_i. \quad (9)$$

Equation (9) is used to control the position of the end-effector as well as the contact force during the interaction with an environment.

## 4 CONTROL OF THE FLEXIBLE LAMBDA ROBOT

The lambda robot controller is separated into feedforward and feedback controller parts. In the feedforward part, the desired signals are calculated based on the robot work space, the joint space, the kinematics, and the dynamics constraints of the robot. The kinematics constraints include the maximum velocity, position of the robot joints, and the closed loop kinematics. The maximum current, the maximum acting force, and the maximum flexible coordinates oscillation amplitude are defined as dynamics constraints, see (Seifried et al., 2011). The feedback control part computes the lambda robot inputs based on the feedback linearization method (Khalil, 2002) using the nonlinear dynamics of the robot, the measured states, and the computed end-effector position.

The feedback controller part based on the application can have three parts, i.e., a position controller, an impedance controller, and the forward kinematics or an observer. In the simplest case, the controller includes only the position controller in the joint space, see (Eberhard and Ansarieshlaghi, 2019). As a next case, the feedback controller includes a position controller and an observer when the joint space controller of the robot is desired, see (Ansarieshlaghi and Eberhard, 2018b). Also, for controlling the end-effector position in the workspace, the position controller and its combination with the forward kinematics is required. In the most complicated case, the feedback controller is a combination of the position controller, the impedance controller, and the forward kinematics part. This combination is used when the contact part of the robot end-effector has an interaction with an environment in the Cartesian space. Therefore, the joint space to the workspace transformation of the system dynamics is required and computed by Equation (9).

Based on the robot work space, the position controller shall generate the robot's inputs in Cartesian space. Therefore, the control law is obtained as

$$\mathbf{u} = -\bar{\mathbf{B}}^{-1}(\bar{\mathbf{f}} + \bar{\mathbf{M}}\mathbf{J}^{-1}(\dot{\mathbf{J}}\dot{\mathbf{q}}_i - \mathbf{K}_P\mathbf{e} - \mathbf{K}_D\dot{\mathbf{e}})). \quad (10)$$

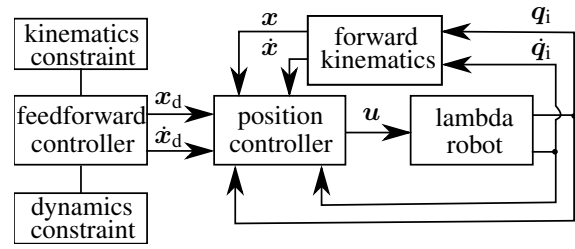


Figure 3: Nonlinear position control structure.

The error and its dynamics are calculated by  $\mathbf{e} = \mathbf{x} - \mathbf{x}_d$  and  $\dot{\mathbf{e}} = \dot{\mathbf{x}} - \dot{\mathbf{x}}_d$  where  $\mathbf{x}_d$  is the desired value of  $\mathbf{x}$ , consequently  $\dot{\mathbf{x}}_d$  is the desired value for  $\dot{\mathbf{x}}$ . The desired trajectories of the end-effector can be computed based on the robot workspace as  $\mathbf{x}_d$  and  $\dot{\mathbf{x}}_d$ . The matrices  $\mathbf{K}_P$  and  $\mathbf{K}_D$  correspond to the weighting of feedback errors and can be designed via the LQR method or tuned by hand. Also, they should satisfy the stability conditions for nonautonomous systems as a uniform stability, based on the Lyapunov theorem.

The lambda robot is an underactuated robot and the input matrix  $\bar{\mathbf{B}}$  is therefore not of full row rank. Thus, the inverse of the input matrix is not so straightforward to calculate. Therefore, the existing left-inverse is used as a pseudo-inverse to yield  $\bar{\mathbf{B}}\bar{\mathbf{B}}^{-1} = \mathbf{I}$ . The vector  $\mathbf{u}$  presents the control input of the robot manipulator and that is the output of the designed position controller based on the feedback linearization method. Figure (3) shows the control structure for controlling the end-effector position in order to track a trajectory in Cartesian space.

The position control for all scenarios as the position or the force/position controller is same as Figure 3. The only difference between the position and hybrid force/position controller is the desired input signal to the controller. This structure is extended to control the contact force to interact with an environment. However, the interactive environment can be a known or an unknown surface.

The robot has only two actuated joints and can just move in the horizontal plane. Hence, the end-effector can only interact with an environment in its movement directions in the horizontal plane. That means that the end-effector shall have contact in one or both directions that the end-effector moves. The position and acting force are dependent and shall be controlled dependently. So the contact force is controlled by using indirect control methods. One of the approaches that is used for indirect force control is the impedance controller method, see (Siciliano and Villani, 1999; Siciliano and Khatib, 2016).

Based on the feedback controller structure presented in Figure 3, the new feedback controller struc-

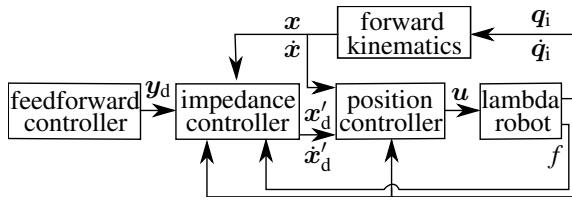


Figure 4: Force/position control structure for interacting with an environment.

ture is developed to control the force and position at the same time. The developed new feedback controller is shown in Figure 4.

The new feedback controller is composed of the position controller, force controller, and the forward kinematics part as a hybrid force/position controller. In Figure 4, the feedforward controller computes the desired values  $y_d$  based on the interactive environment that can be a known or an unknown surface. For a known scenario, the desired values  $y_d$  are the position of the surface  $x_d$ , the moving velocity on the surface  $\dot{x}_d$ , and the magnitude of the acting force on the surface  $f_d$  in Cartesian space. The desired values for the unknown case are the magnitude of the moving velocity  $v_d$  and the acting force  $f_d$  on the surface.

The impedance part of the feedback controller computes a new desired position and velocity of the robot's end-effector based on the desired values by the feedforward controller, the measured states  $q_i$  and  $\dot{q}_i$ , the contact force  $f$ , and the computed or observed position of the contact part by the forward kinematics. The position controller acts as the last part in Figure 3 based on its input signals and the dynamics model of the robot.

In order to interact with an environment, a tool that is shown in Figure 5 is designed and installed on the end-effector in Figure 2.

The basic idea of the designed tool is to control the contact force during moving on the surface. Therefore, based on the robot configuration and its degrees of freedom, the contact part's force should be defined as a function of the end-effector position. Thus, the tool is designed to be a transfer function, to convert the interaction force of the contact part to the end-effector position displacement. This transfer tool is designed such that the acting force accurately and reliably is transferred to the force sensor. The tool includes a body for interacting as a contact part, a movable body which is connected to a spring for transferring the contact force, a force sensor to measure the interacting force, and a structure to constrain the spring in the force direction and to avoid its bending and deformation. Also, for the movable body, a safety stop is considered to limit the measured force and protect the force sensor.

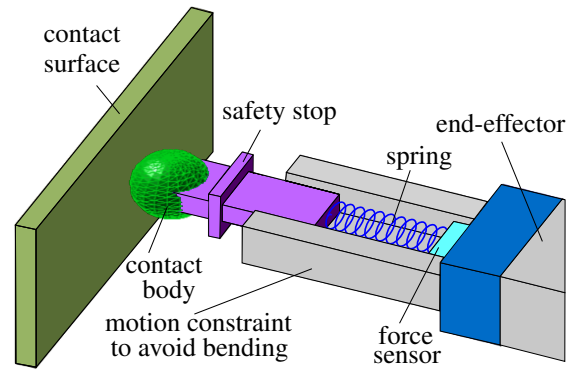


Figure 5: Designed tool for interacting with an environment.

## Impedance Control

Impedance control is a method used for indirect force regulation. The impedance refers the dynamic relation of the motion and contact force of the manipulator during an interaction with an object. It means that the impedance controller transfers the contact force as a function of the contact part's position and then, the position controller regulates it.

In this work, for modeling the impedance part only a spring with stiffness  $k$  is used. The free length of the designed tool is  $l_0$ . For controlling the contact part's position and its acting force, the end-effector position shall be controlled. For this goal, based on the desired input  $y_d$ , measurement signals  $y = [q_i, \dot{q}_i, f]^T$ , and the feedforward kinematics, the new desired end-effector position and velocity are obtained as

$$x'_d = g_1(y_d, y, x, k, l_0), \quad (11a)$$

$$\dot{x}'_d = g_2(y_d, y, \dot{x}). \quad (11b)$$

The important point in this work is that the environment model is unknown and we do not have any information about its shape. The environment can be flexible, deformable, movable, or compressible. The only difference between a known and an unknown environment for this work is, when the position and moving velocity on the surface is known, the environment is named known. For an unknown environment, only the magnitude of moving velocity is given and based on the measured force, the impedance part can distinguish wherever that the contact body is in contact or not. Based on this idea, it computes the new desired values  $(x'_d, \dot{x}'_d)$ .

After introducing the environments that the robot can interact with, now parameters that are used for updating the new desired values are defined. The parameters are determined based on the inputs of the functions  $g_1$  and  $g_2$  of Equation (11) in Figure 6.

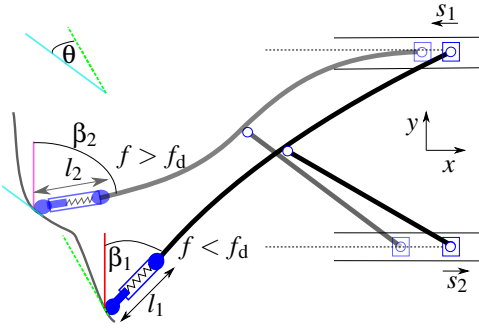


Figure 6: Schematic view of the lambda robot in contact with an environment.

Figure 6 shows a schematic view of the lambda robot and its designed tool in interacting with an environment. The designed contact tool's length can change based on the acting force. The angles  $\beta_1$  and  $\beta_2$  are between the  $y$ -direction of the global coordinate system and the robot end-effector in two configurations. It is calculated by

$$\beta = g_4(q_i) = \frac{\pi}{2} - (\alpha_1 + r q_e). \quad (12)$$

The constant  $r$  is the gain for the elastic rotation and displacement of the long flexible link. The angle  $\theta$  is computed based on the position of the robot end-effector at the current sample time  $t$  and the previous sample time  $t - \Delta t$

$$\begin{aligned} \theta &= g_3(\mathbf{x}_t, \mathbf{x}_{t-\Delta t}) \quad (13) \\ &= \arctan\left(\frac{x_{x_t}}{x_{y_t}}\right) - \arctan\left(\frac{x_{x_{t-\Delta t}}}{x_{y_{t-\Delta t}}}\right). \end{aligned}$$

In Equation (14a),  $x_{x_t}$  is the end-effector position at the current time in the  $x$ -direction and  $x_{y_t}$  is in the  $y$ -direction. For previous sample time, the end-effector position in the  $x$ -direction and  $y$ -direction are  $x_{x_{t-\Delta t}}$  and  $x_{y_{t-\Delta t}}$ .

The new desired position and velocity of the end-effector for a known case using Equation (11) can be rewritten using the new defined parameters in Equations (12) and (13) for the next sample time  $t + \Delta t$  as

$$\mathbf{x}'_d(t + \Delta t) = \mathbf{g}_1(\beta, f_d, f, \mathbf{x}_d, k, l_0) \quad (14a)$$

$$\dot{\mathbf{x}}'_d(t + \Delta t) = \mathbf{g}_2(\theta, \dot{\mathbf{x}}, \dot{\mathbf{x}}_d). \quad (14b)$$

In this case, the new desired position  $\mathbf{x}'_d$  and the function  $\mathbf{g}_1$  are computed using Equation (14a) as

$$\mathbf{x}'_d = \mathbf{g}_1 = \mathbf{x}_d - \begin{bmatrix} l_0 \sin(\beta) \\ l_0 \cos(\beta) \end{bmatrix} + \frac{\mathbf{P}_j}{k} \begin{bmatrix} f_e \sin(\beta) \\ f_e \cos(\beta) \end{bmatrix}. \quad (15)$$

In Equation (15),  $f_e$  is the regulation force error as  $f_e = f_d - f$  and the matrix  $\mathbf{P}_j$  presents the design gain.

The subscript  $j$  is related to the different situations are shown in Figure 6 and is a function of the force regulation's amplitude error  $f_e$  and its sign. Using difference gain matrices for difference conditions in a gain scheduling method improves the position tracking and force regulation performances and adapts the robot to the new interaction situation.

Also, to increase the accuracy of the position tracking and improve the force regulation tasks, the function  $\mathbf{g}_2$  in Equation (14b) is defined by

$$\begin{aligned} \dot{\mathbf{x}}'_d &= \mathbf{g}_2 \quad (16) \\ &= \begin{bmatrix} \cos(\theta) & \sin(\theta) \\ \sin(\theta) & \cos(\theta) \end{bmatrix} \dot{\mathbf{x}}_d + \mathbf{A}_n \begin{bmatrix} \cos(\theta) & \sin(\theta) \\ \sin(\theta) & \cos(\theta) \end{bmatrix} \dot{\mathbf{e}}. \end{aligned}$$

The matrix  $\mathbf{A}_n$  is the design gain. The subscript  $n$  depends on the magnitude of the velocity error  $\|\dot{\mathbf{e}}\|$  and adapts the robot end-effector velocities for different contact configuration.

For an unknown interaction, the new desired values are computed as

$$\mathbf{x}'_d = \mathbf{x} + \frac{\mathbf{P}_j}{k} \begin{bmatrix} f_e \sin(\beta) \\ f_e \cos(\beta) \end{bmatrix}. \quad (17)$$

For next sample time, the new velocity of the end-effector is calculated

$$\dot{\mathbf{x}}'_d = \begin{bmatrix} v_d \sin(\theta) \\ v_d \cos(\theta) \end{bmatrix} + \mathbf{A}_n \begin{bmatrix} \cos(\theta) & \sin(\theta) \\ \sin(\theta) & \cos(\theta) \end{bmatrix} \mathbf{e}_v, \quad (18)$$

where  $v_d$  is the magnitude of the moving velocity on the surface and it can be a constant or function of time or the end-effector position. The velocity error vector  $\mathbf{e}_v$  is the difference of the measured and desired velocity and is computed using  $\dot{\mathbf{x}} = [v_x, v_y]^T$  as

$$\mathbf{e}_v = \begin{bmatrix} v_d \sin(\theta) \\ v_d \cos(\theta) \end{bmatrix} - \begin{bmatrix} v_x \\ v_y \end{bmatrix}. \quad (19)$$

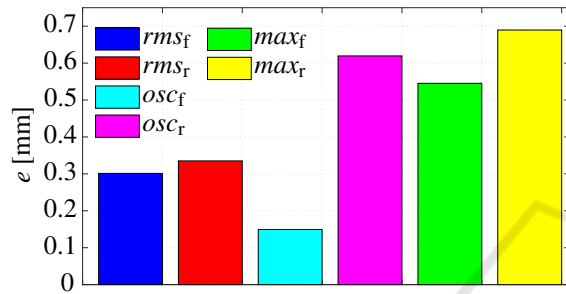
The impedance controller obtains the next position and velocity of the end-effector based on the interacted environment and the defined goal for each interaction. It means that for the known interaction task, controlling the position of the acting force has a great importance and regulating the acting force in the specified positions is desired. In contrast, for the unknown case, controlling the specified desired acting force during moving along the surface is desired.

## 5 SIMULATION RESULTS

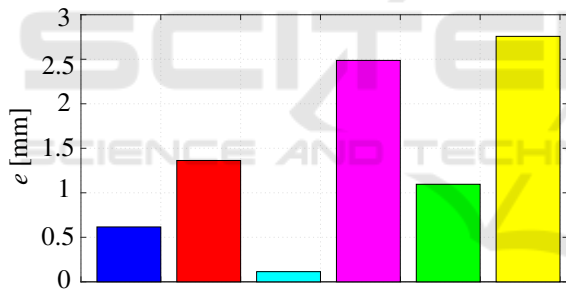
To validate the designed nonlinear controller, some tasks in the Cartesian space are specified as the trajectory tracking by the position controller of the robot end-effector and interacting with a surface via the hybrid force/position controller.

The nonlinear controllers are designed based on the flexible model with five degrees of freedom and the rigid model with four degrees of freedom of the lambda robot. The controllers are implemented on the robot model with eleven degrees of freedom because the previous researches and testing on the lambda robot in (Ansarieshlaghi and Eberhard, 2018b; Eberhard and Ansarieshlaghi, 2019) show that the real system behavior is very close to this model.

For pure position control, the controllers track a line trajectory with low and high speed. The results are shown in Figure 7.



(a) Tracking the line trajectory with low speed.



(b) Tracking the line trajectory with high speed.

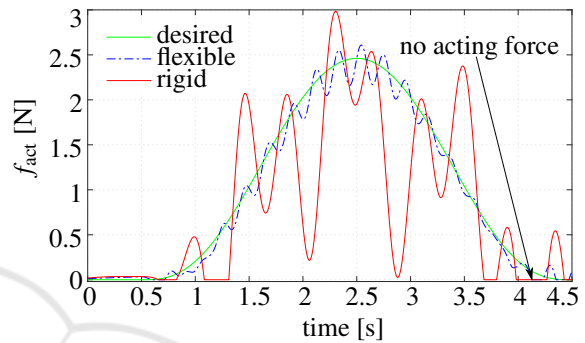
Figure 7: Comparison of the end-effector trajectory tracking results based on the rigid (r) and flexible (f) controllers. In these comparisons, the root-mean-squared (rms), maximum tracking error (max), and maximum oscillation amplitude (osc) are used as benchmarks.

Based on the simulation results of two controllers, the flexible model based controller tracks the trajectory with higher accuracy and less oscillation amplitude than the rigid model based, see Figure 7 for both tracking velocities. The difference of controllers performances is increased when the end-effector tracks a trajectory with high speed in Figure 7b. Also, the results show the end-effector position controller based on the flexible model can track a trajectory with less than 1% normalized root mean square error.

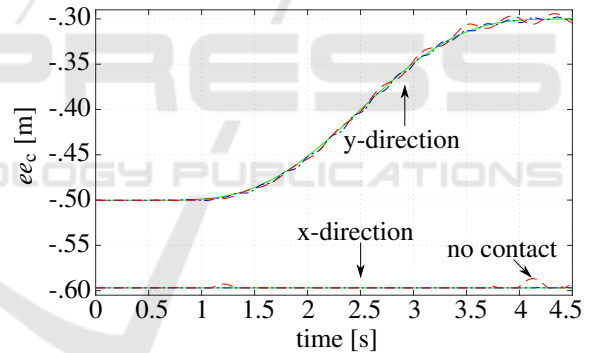
To validate the hybrid force/position controller, in a first scenario, the robot interacts with a known

flat surface during high speed moving. The spring stiffness for this scenario, in Equations (15) is  $k = 100 \text{ N/m}$ . Figure 8 shows interaction results, e.g., tracking the surface and the acting force on the surface by the robot contact tool.

For interacting with a known flat environment, the maximum normalized root mean square error of the flexible based impedance controller for moving in the desired position and regulating acting force on the surface are used as benchmarks and these are 1% and 5%, respectively, see Figures 8b and 8a.



(a) Acting force on a known surface in fast movement.

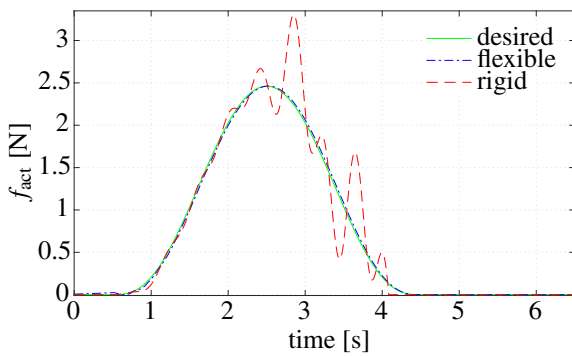


(b) Contact part position on a known surface in fast movement.

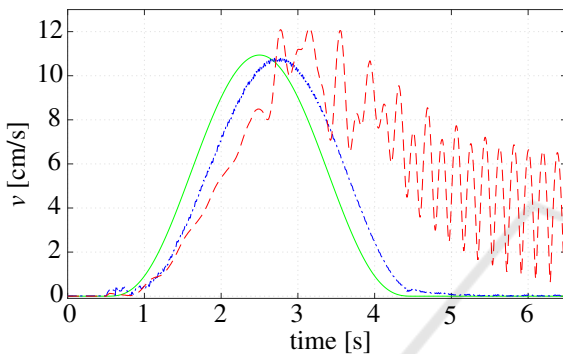
Figure 8: Comparison of the robot's interaction with a known surface. Flexible presents nonlinear controller based on the flexible model and rigid shows the result of the controller based on the rigid model.

These results show that the hybrid force/position controller is able to apply the force at the desired position with high accuracy.

As the next scenario, a more difficult and challenging task is investigated where the robot is interacting with an unknown environment. The used spring for impedance modeling for the contact tool, in Equations (17) has same value as in the known case. Figure 9 shows the robot manipulation results. In contrast of the known case, the controller goal is related to the acting force regulation during moving on a flat



(a) Acting force on an unknown surface in fast movement.



(b) End-effector tracking velocity on an unknown surface in fast moving.

Figure 9: Comparison the robot interaction with an unknown surface. Flexible presents nonlinear controller based on the flexible model and rigid show result of the controller based on the rigid model.

surface.

For interacting with an unknown environment, the moving with desired velocity and regulating the acting force on the surface are investigated. The results show the flexible model based controller achieved drastically better performance than the rigid model based. Also, the interaction results show that the flexible controller can move on an unknown surface during force regulating with more than 99% accuracy and at minimum 88% for tracking moving velocity.

The performance of the force/position controller in each interaction scenario shows that the flexible model based controller reaches their desired goals successfully and overcome to the challenges.

## 6 CONCLUSIONS

In this paper, a high performance end-effector position controller and its combination with an impedance controller are presented for a flexible parallel robot manipulator to interact with an environment. The de-

signed position controller based on the independent system coordinates computes the robot's input using the measurable states of the system, the obtained, and the desired position and velocity of the end-effector. The nonlinear feedback controller is extended with an impedance part in order to regulate the contact force, too. The simulation results on the lambda robot model show that the nonlinear controllers based on the flexible model have drastically better performance than the rigid model based controllers. Also, the hybrid force/position controller did all complicated tasks with high accuracy and successfully overcame to all challenges, too.

For future work, the designed controllers, i.e., the position and impedance controller will be tested on the real robot and their performance will be investigated.

## ACKNOWLEDGEMENTS

This research presented in the Cluster of Excellence in Simulation Technology SimTech at the University of Stuttgart and is partially funded by the Landesgraduierten kolleg Baden-Württembergs. The authors appreciate these discussions.

## REFERENCES

- Ansarieshlaghi, F. and Eberhard, P. (2017). Design of a nonlinear observer for a very flexible parallel robot. In *Proceedings of the 7th GACM Colloquium on Computational Mechanics for Young Scientists from Academia and Industry*, Stuttgart, Germany.
- Ansarieshlaghi, F. and Eberhard, P. (2018a). Experimental study on a nonlinear observer application for a very flexible parallel robot. *International Journal of Dynamics and Control*, doi:10.1007/s40435-018-0467-2.
- Ansarieshlaghi, F. and Eberhard, P. (2018b). Trajectory tracking control of a very flexible robot using a feedback linearization controller and a nonlinear observer. In *Proceedings of 22nd CISM IFToMM Symposium on Robot Design, Dynamics and Control*, Rennes, France.
- Burkhardt, M., Holzwarth, P., and Seifried, R. (2013a). Inversion based trajectory tracking control for a parallel kinematic manipulator with flexible links. In *Proceedings of the 11th International Conference on Vibration Problems*, Lisbon, Portugal.
- Burkhardt, M., Seifried, R., and Eberhard, P. (2013b). Aspects of symbolic formulations in flexible multibody systems. *Journal of Computational and Nonlinear Dynamics*, 9(4):041013-1-041013-8.
- Burkhardt, M., Seifried, R., and Eberhard, P. (2014). Experimental studies of control concepts for a parallel ma-



- nipulator with flexible links. In *Proceedings of the 3<sup>rd</sup> Joint International Conference on Multibody System Dynamics and the 7<sup>th</sup> Asian Conference on Multibody Dynamics*, Busan, Korea.
- Eberhard, P. and Ansarieshlaghi, F. (2019). Nonlinear position control of a very flexible parallel robot manipulator. In *Proceedings ECCOMAS Thematic Conference on Multibody Dynamics*, Duisburg, Germany (accepted for publication).
- Endo, T., Sasaki, M., Matsuno, F., and Jia, Y. (2017). Contact-force control of a flexible timoshenko arm in rigid/soft environment. *IEEE Transactions on Automatic Control*, 62(5):2546–2553.
- Feliu-Talegon, D., Feliu-Batlle, V., Tejado, I., Vinagre, B. M., and HosseinNia, S. H. (2019). Stable force control and contact transition of a single link flexible robot using a fractional-order controller. *ISA transactions*.
- Hogan, N. (1985). Impedance control: An approach to manipulation: Part II—Implementation. *Journal of Dynamic Systems, Measurement, and Control*, 107(1):8–16.
- Jung, S., Hsia, T. C., and Bonitz, R. G. (2004). Force tracking impedance control of robot manipulators under unknown environment. *IEEE Transactions on Control Systems Technology*, 12(3):474–483.
- Kamikawa, Y., Enayati, N., and Okamura, A. M. (2018). Magnified force sensory substitution for telemanipulation via force-controlled skin deformation. In *IEEE International Conference on Robotics and Automation (ICRA)*, pages 1–9, Brisbane, Australia.
- Khalil, H. K. (2002). *Nonlinear systems*, volume 3. Prentice hall, Upper Saddle River.
- Li, Y., Ganesh, G., Jarrassé, N., Haddadin, S., Albuschaeffer, A., and Burdet, E. (2018). Force, impedance, and trajectory learning for contact tooling and haptic identification. *IEEE Transactions on Robotics*, 34(5):1170–1182.
- Luh, J., Fisher, W., and Paul, R. (1983). Joint torque control by a direct feedback for industrial robots. *IEEE Transactions on Automatic Control*, 28(2):153–161.
- Morlock, M., Burkhardt, M., Schröck, C., and Seifried, R. (2017). Nonlinear state estimation for trajectory tracking of a flexible parallel manipulator. *IFAC-PapersOnLine*, 50(1):3449–3454.
- Morlock, M., Burkhardt, M., and Seifried, R. (2016). Control of vibrations for a parallel manipulator with flexible links - concepts and experimental results. In *MOVIC & RASD, International Conference*, Southampton, England.
- Sandoval, J., Su, H., Vieyres, P., Poisson, G., Ferrigno, G., and Momi, E. D. (2018). Collaborative framework for robot-assisted minimally invasive surgery using a 7-dof anthropomorphic robot. *Robotics and Autonomous Systems*, 106:95–106.
- Schindlbeck, C. and Haddadin, S. (2015). Unified passivity-based cartesian force/impedance control for rigid and flexible joint robots via task-energy tanks. In *IEEE international conference on robotics and automation (ICRA)*, pages 440–447, Seattle, Washington. IEEE.
- Seifried, R., Burkhardt, M., and Held, A. (2011). Trajectory control of flexible manipulators using model inversion. In *Proceedings of the ECCOMAS Thematic Conference on Multibody Dynamics*, Brussels, Belgium.
- Siciliano, B. and Khatib, O., editors (2016). *Springer Handbook of Robotics*. Springer Heidelberg.
- Siciliano, B. and Villani, L. (1999). *Robot Force Control*. Springer Science & Business Media.
- Suarez, A., Giordano, A. M., Kondak, K., Heredia, G., and Ollero, A. (2018). Flexible link long reach manipulator with lightweight dual arm: Soft-collision detection, reaction, and obstacle localization. In *IEEE International Conference on Soft Robotics (RoboSoft)*, pages 406–411. IEEE.
- Vogel, J., Haddadin, S., Jarosiewicz, B., Simeral, J. D., Bacher, D., Hochberg, L. R., Donoghue, J. P., and van der Smagt, P. (2015). An assistive decision-and-control architecture for force-sensitive hand–arm systems driven by human–machine interfaces. *The International Journal of Robotics Research*, 34(6):763–780.